Electronic Supplementary Information

Electrospun $BiVO_4$ Nanobelts with Tailored Structures and Their Enhanced Photocatalytic/photoelectrocatalytic Activities

Huabing Liu,[a b] Weiyou Yang ,[a] Lin Wang,[a] Huilin Hou [a] and Fengmei Gao [a*]*

[a] Institute of Materials, Ningbo University of Technology, Ningbo City, 315016, P.R. China.

[b] School of Materials Science and Engineering, Shanghai Jiao Tong University, Shanghai City, 200240, P.R. China.

Corresponding Author E-mails: houhuilin86@163.com (H. Hou)

fmgao@163.com (F. Gao)

Tel: +86-574-87080966

Fax: +86-574-87081221

Experimental

The tailored $BiVO_4$ nanobelts were fabricated by a typical electrospinning method, which was performed through electrospinning the solution of high-molecular-weight polyvinylpyrrolidone (PVP-K90 MW ≈ 1300000, Aladdin, Shanghai, China), low-molecular-weight polyvinylpyrrolidone (PVP-K30 MW ≈ 40000, Aladdin, Shanghai, China) and $Bi(NO_3)_3 \cdot 5H_2O$ and $VO(acac)_2$ followed by calcination in air. The raw materials of PVP-K90, PVP-K30, Bi $(NO_3)_3 \cdot 5H_2O$ (Aladdin, Shanghai, China), $VO(acac)_2$ (Aladdin, Shanghai, China) and DIPA (Adamas, Shanghai, China) were commercially available and used directly without further purification.

In a typical experimental procedure, PVP-K90 and PVP-K30 with the different mass ratio were firstly dissolved in a mixed solvent containing of 2.0 g acetic, 2.5 g ethanol and 2.5 g N,N-dimethyformamide (DMF) with vigorously stirring for 3 h. Then, 1.21 g of Bi $(NO_3)_3 \cdot 5H_2O$ and 0.662 g $VO(acac)_2$ (Aldrich) were added into the above solution, and continue to be magnetically stirred for 3 h. The resultant solution was then transformed into a plastic syringe with a stainless steel nozzle (anode, diameter: 0.412 mm). The tip of the stainless steel nozzle was placed in the front of a metal cathode (collector) with a fixed distance of 20 cm between the nozzle and the collector. A columnar barrel covering by the aluminum foil was acted as the cathode collector, and an electrical potential of 12 kV was applied for electrospinning precursor fibers. The as-spun polymer fibers were dried in a constant temperature oven (fixed at 80 °C). Subsequently, the obtained samples were located in a quartz crucible and placed at the center of a chamber furnace. Finally, the precursor fibers were heated up to the desired temperature of 500 °C with a heating rate of 4 °C/min and maintained there for 1 h in air, followed by furnace cool to ambient temperature. For comparison, four precursor solutions were prepared with different mass ratio of PVP-K90 and PVP-K30 compositions and keeping the others at a constant amount, as detailed shown in Table S1. The resultant products were referred to as Sample A-D, respectively.

The obtained products were characterized with X-ray powder diffraction (XRD, D8 Advance, Bruker, Germany) with Cu Kα radiation (λ=1.5406 Å), The optical properties of the samples were characterized using a UV-Vis scanning spectrophotometer (U-3900, Japan) (DRS), in which $BaSO_4$ was employed as the internal reflectance standard. Raman spectrometer (InVia, Renishaw, UK), field emission scanning electron microscopy (FESEM, S-4800, Hitachi, Japan), and high-resolution

transmission electron microscopy (HRTEM, JEM-2010F, JEOL, Japan) equipped with the energy dispersive X-ray spectroscopy (EDX, Quantax-STEM, Bruker, Germany). The BET specific surface area of the as-prepared $BiVO_4$ photocatalysts were characterized using N_2 adsorption at -195.8 °C on a specific surface area analyser (ASAP 2020 HD88, Micromeritics, USA).

The photocatalytic activities of the as-prepared samples were evaluated by the photodegradation of Rhodamine B (RhB) in a reactor with a volume of 100 ml under the visible light irradiation. The irradiation source is a 350 W Xe lamp with a 420 nm cutoff filter. The photocatalytic activities of the sample were judged by measuring the loss of SRB in aqueous solution. The initial volume and concentration of RhB was 50 ml and 2.5×10^{-5} M, respectively. Prior to irradiation, the suspensions were magnetically stirred in dark for 30 minutes to ensure the establishment of absorption-desorption equilibrium between the catalyst and the dye. The concentration of RhB was analyzed by recording the absorption band maximum in the UV-Vis spectra of RhB using a spectrophotometer (U-3900, Hitachi, Japan). In comparison, the photocatalytic performances over the commercial P25 photocatalyst were further studied under the same conditions.

The photoelectrocatalytic (PEC) water splitting performances of all the three samples were measured using a standard three-electrode system. The cell was composed of a KCl saturated Ag/AgCl electrode as reference (0.1976 VRHE at 25 ℃), a Pt foil as the cathode and the electrospun products electrode as the pho-toanode. The $BiVO_4$ materials were spin-coated on the fluorine-doped tin oxide (FTO) glass (Sigma–Aldrich). Before being spin-coated, the substrates were ultrasonically pre-cleaned in acetone, de-ionized water, and ethanol for 30 minutes respectively, and then dried in a constant temperature oven (fixed at 90 °C). In addition, all of the electrodes were positioned as close together as possible and these positions were the same for every sample measurement and the anodic photoresponses were measured under simulated AM 1.5 irradiation. Then, the currents were measured by a potentiostat in a 0.5 M $NaSO_4$ electrolyte (pH=7.0).

Table S1. Composition details of the five solutions used for electrospinning polymer precursor fibers

Sample	$Bi(NO_3)_3.5H_2O$ (g)	$VO(acac)_2$ (g)	Alcohol (g)	Aceticacid (g)	DMF (g)	K90 (g)	K30: K90
A	1.21	0.662	2	2.5	2.5	0.4	1:1
B	1.21	0.662	2	2.5	2.5	0.4	2:1
C	1.21	0.662	2	2.5	2.5	0.4	3:1
D	1.21	0.662	2	2.5	2.5	0.4	4:1

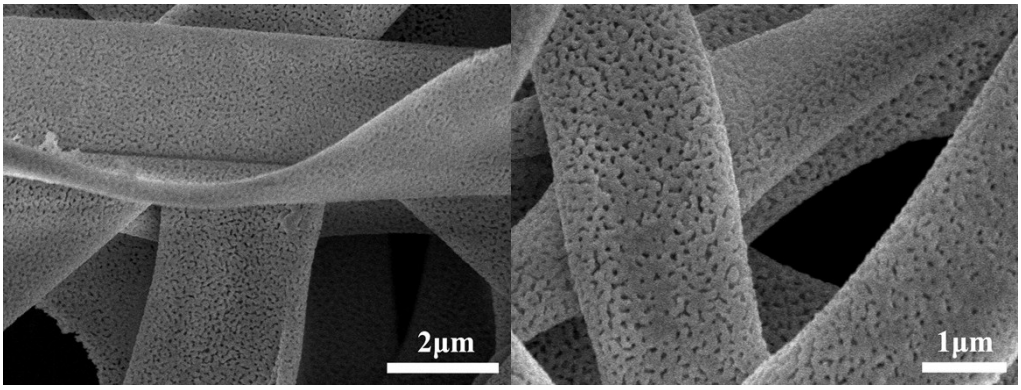

Fig. S1 Typical SEM images of calcined nanobelts of Sample C (PVP-K30: PVP-K90=3:1) under different magnifications.

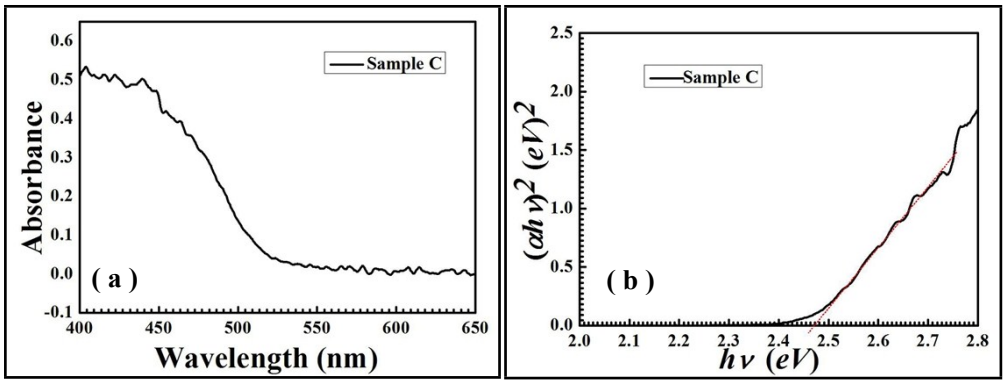

Fig. S2 (a) UV-vis diffuse reflectance spectra of the mesoporous nanofibers of Sample C (PVP-K30: PVP-K90=3:1). **(b)** the plot of $(Ahv)^2$ vs. hv.

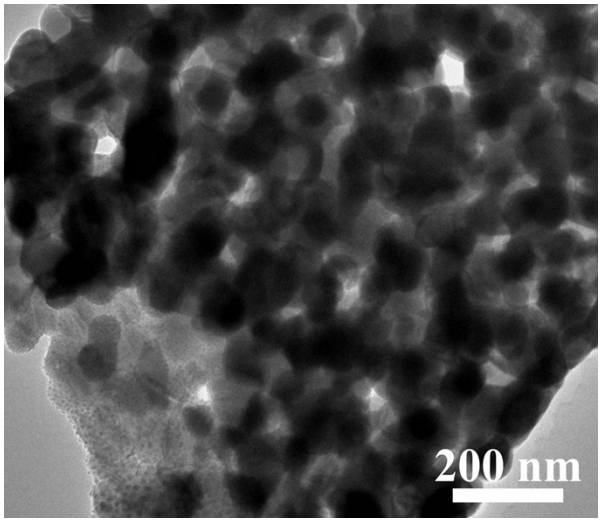

Fig. S3 Closer TEM observation of the nanobelt body under high magnification

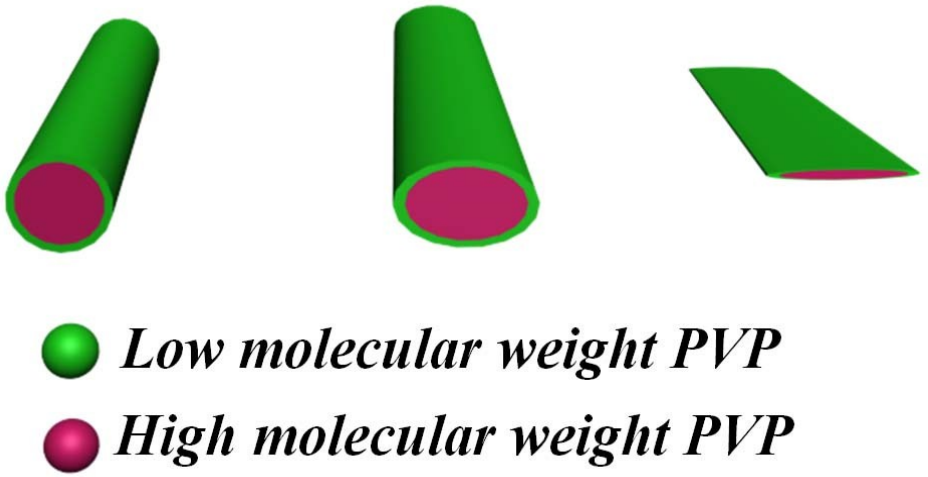

Fig. S4 Schematic illustration of the formation of $BiVO_4$ nanobelts

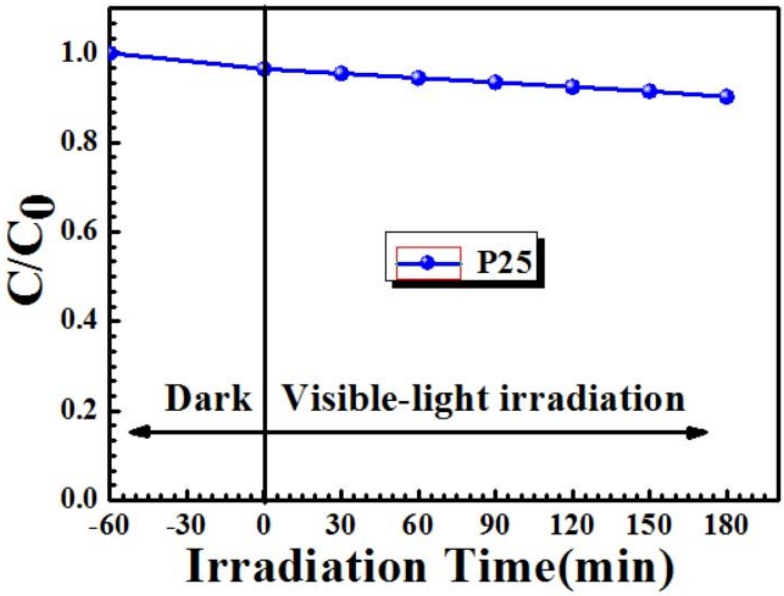

Fig. S5 Photocatalytic degradation of RhB over the P25 photocatalysts under visible light irradiation..

Table S2. Summary of the BET Surface area value of the three sample photocatalysts

Sample	Morphology	BET Surface area (m^2/g)
A	Nanofibers	5.3
C	Nanobelts	14.4
D	Sheets	9.4

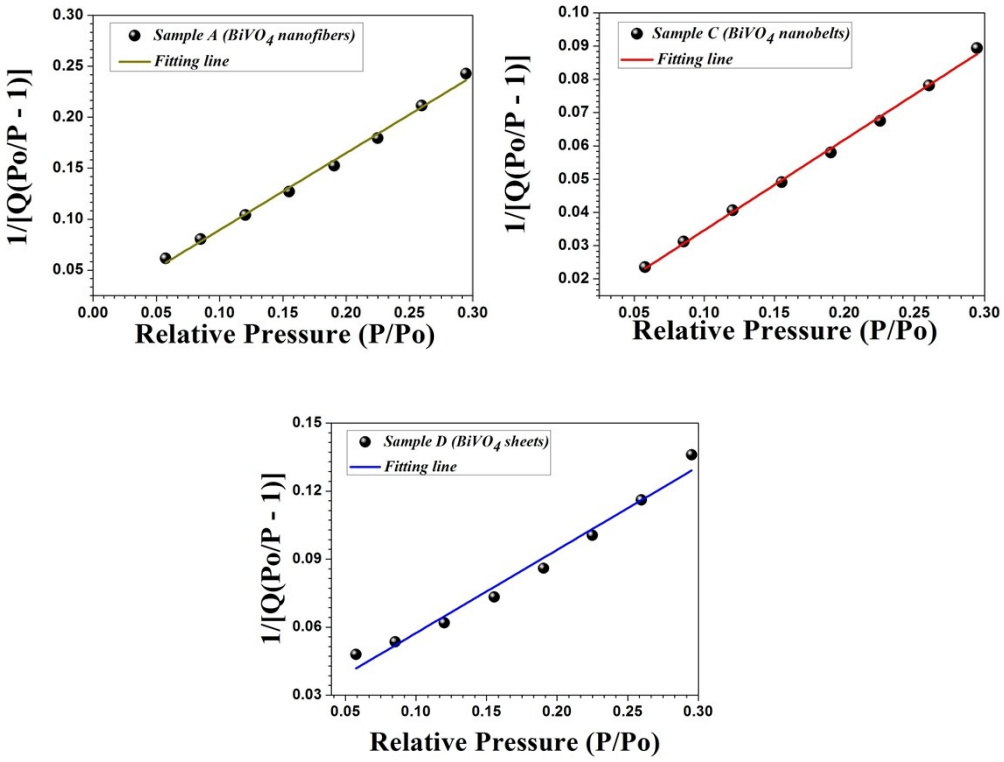

Fig. S6 BET Surface area plot of the three sample photocatalysts.